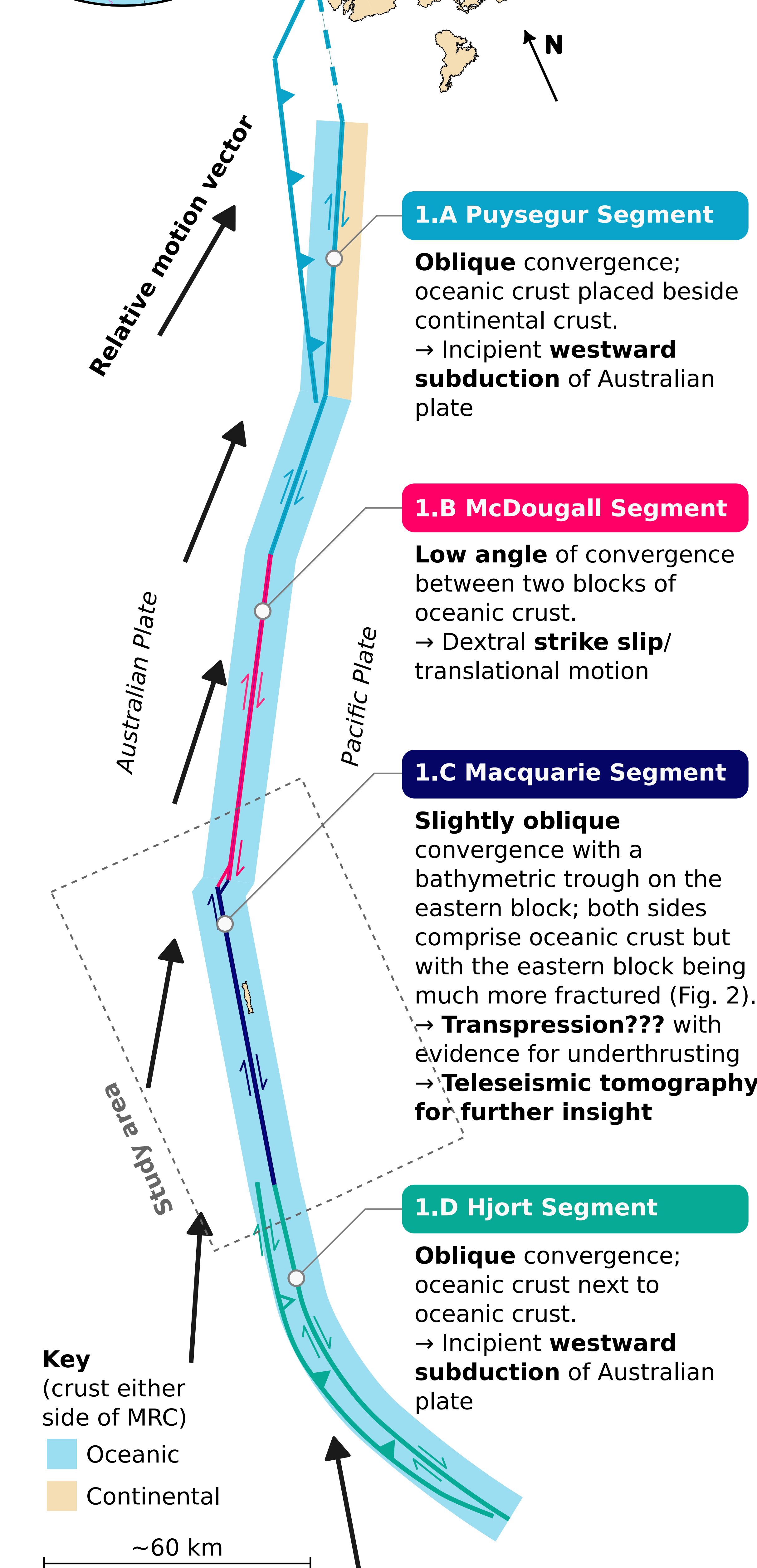


Revealing the Australian-Pacific Plate Boundary Beneath Macquarie Island with Teleseismic Tomography

Y. Li, N. Rawlinson, C. Lü, T. O'Hara, T. Winder, H. Tkalčić, M. Coffin & J. Stock
 ✉y.li@esc.cam.ac.uk



1.A Puysegur Segment

Oblique convergence; oceanic crust placed beside continental crust.
 → Incipient **westward subduction** of Australian plate

1.B McDougall Segment

Low angle of convergence between two blocks of oceanic crust.
 → Dextral **strike slip/** translational motion

1.C Macquarie Segment

Slightly oblique convergence with a bathymetric trough on the eastern block; both sides comprise oceanic crust but with the eastern block being much more fractured (Fig. 2).
 → **Transpression???** with evidence for **underthrusting**
 → **Teleseismic tomography** for further insight

1.D Hjort Segment

Oblique convergence; oceanic crust next to oceanic crust.
 → Incipient **westward subduction** of Australian plate

1. Introduction

The **Macquarie Ridge Complex (MRC)** comprises four segments (1.A to 1.D) and marks the plate boundary separating the **Australian** and **Pacific** plates south of New Zealand^[1]. The MRC hosts diverse **tectonic regimes** (Fig. 1) controlled principally by the **angle** between the relative plate motion vector and plate boundary orientation^[2,3].

We use **teleseismic** data from a temporary seismometer network (Fig. 2) to produce a **P-wave velocity** model of the mantle beneath Macquarie Island via **seismic tomography**.

2. Data and Methods

Seismometer network^[7] (Oct 2020 to Nov 2021; Fig. 2):
 • 15 temporary **ocean bottom seismometers (OBSS)**
 • 5 temporary and 1 permanent **land stations**

OBSS data is very noisy, so ATaCR^[8,9] was used to **denoise** the data (Fig. 3). After denoising, **65 phase arrivals** (Fig. 4) could be used for teleseismic tomography.

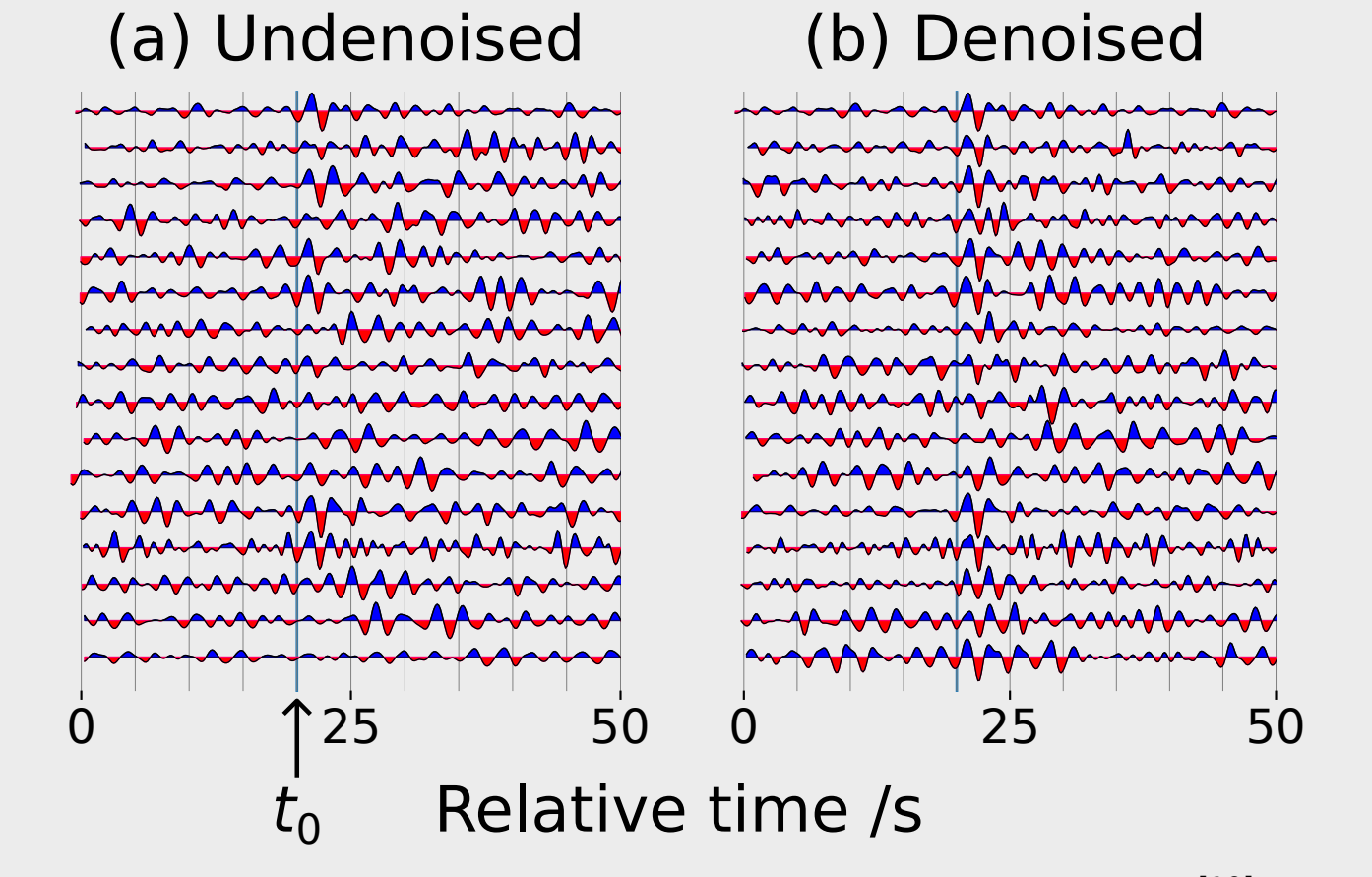


Figure 3 Alignments generated by adaptive stacking^[10] for (a) undenoised and (b) ATaCR denoised waveforms. t_0 is the predicted P arrival time for event 2021-01-08T05:01:04.07.

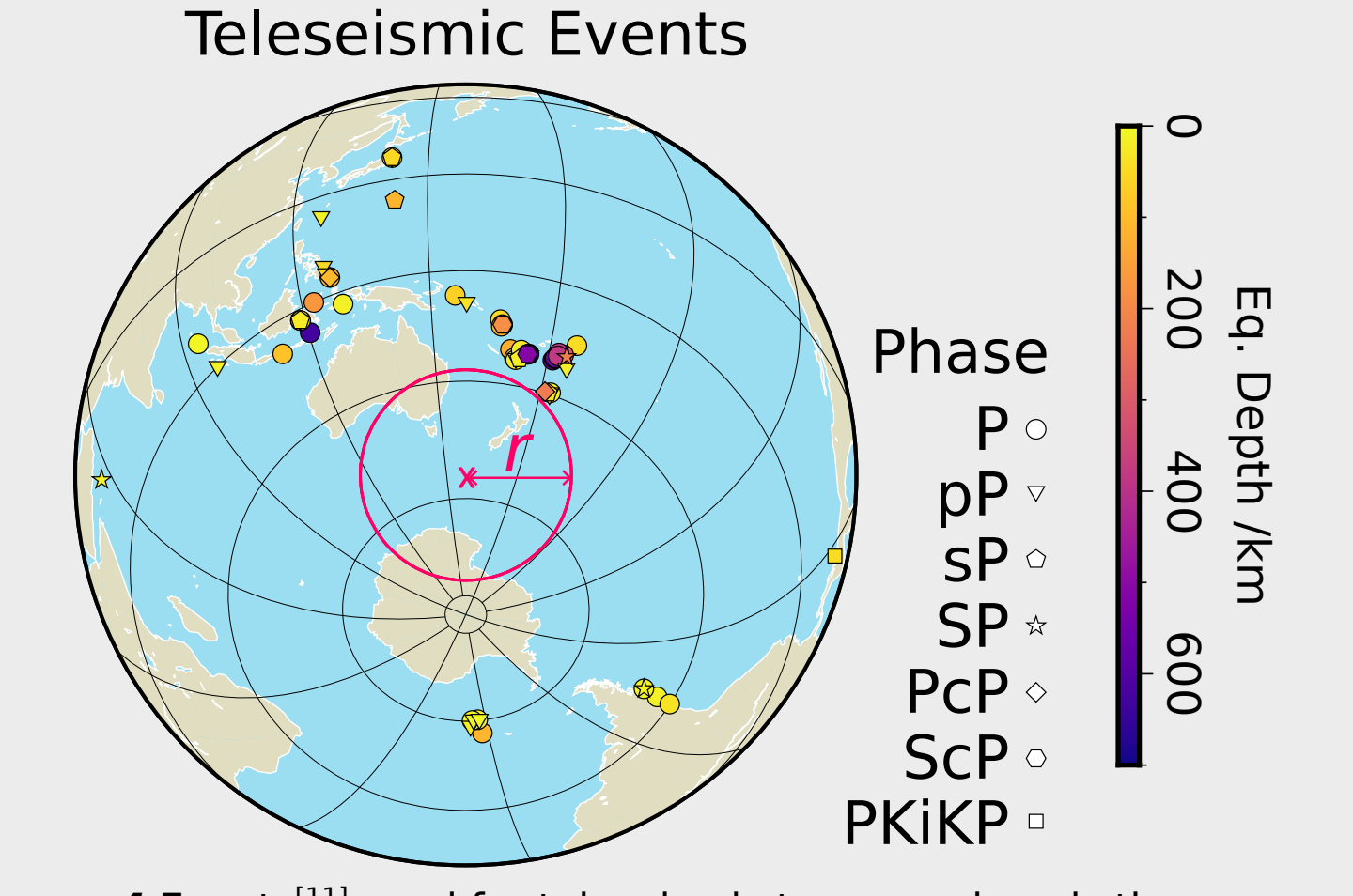


Figure 4 Events^[11] used for teleseismic tomography. r is the teleseismic threshold (27°) from the center of the study region.

3. Results

Good checkerboard recovery at lithospheric mantle depths. Velocity model reveals **contrast across plate boundary**: lithosphere to W is ~0.4 km/s faster.

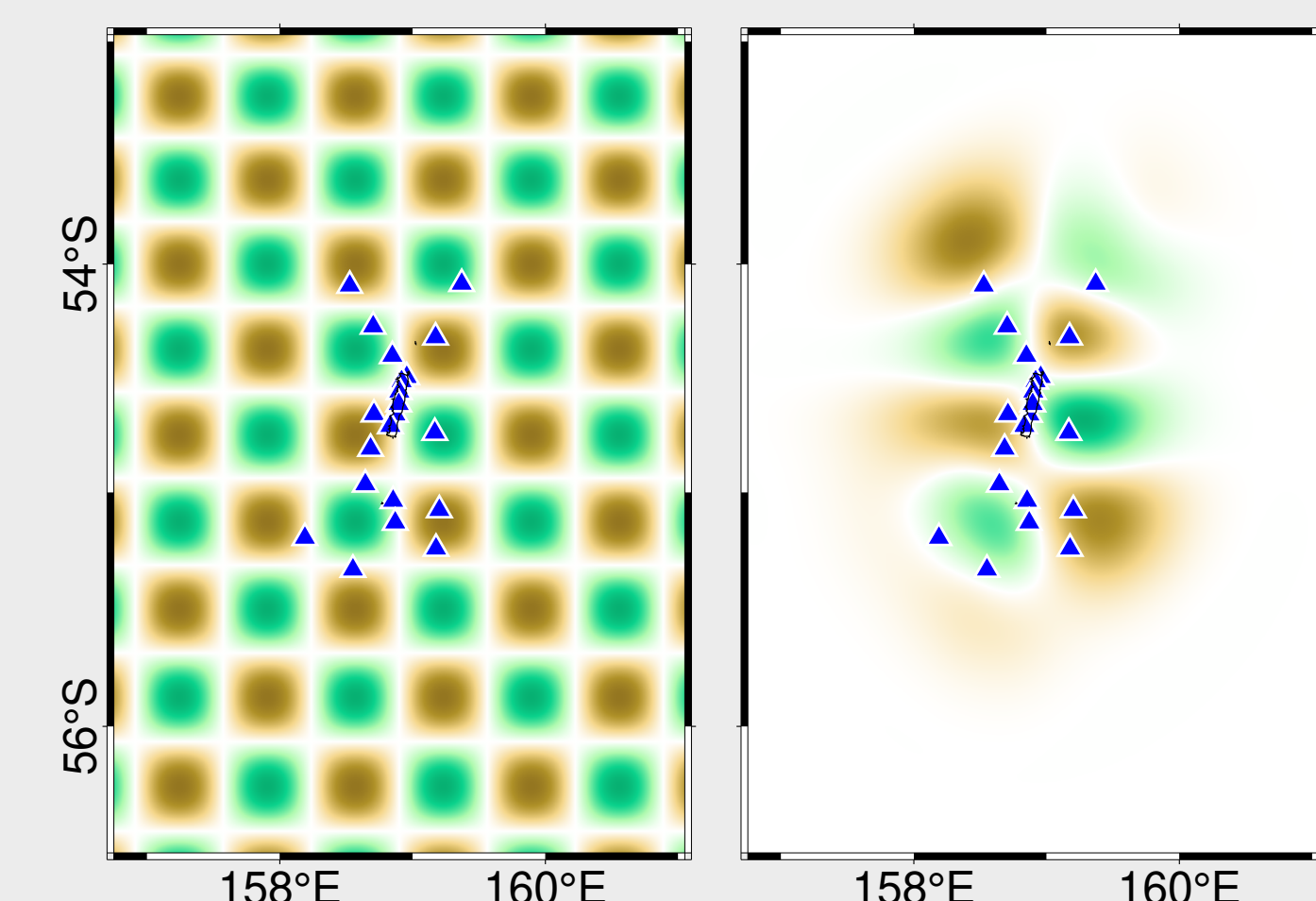


Figure 5 Checkerboard recovery test at 30 km depth. Left: true velocity structure. Right: recovered velocity structure. Stations are plotted as blue triangles.

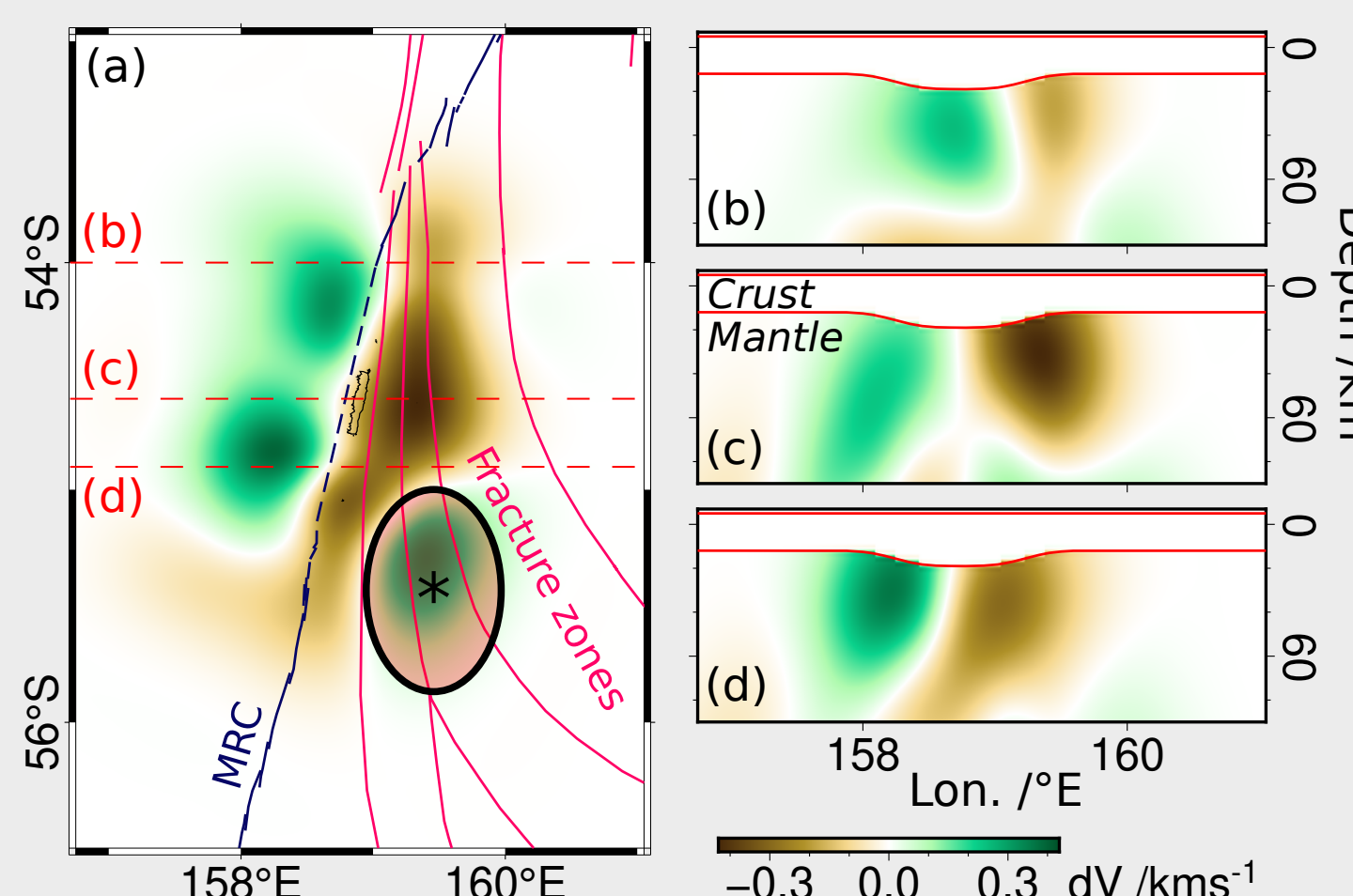


Figure 6 Recovered velocity model at (a) 30 km depth, (b) 54.0°S, (c) 54.6°S and (d) 54.9°S. *Feature constrained by singular station and thus not robust.

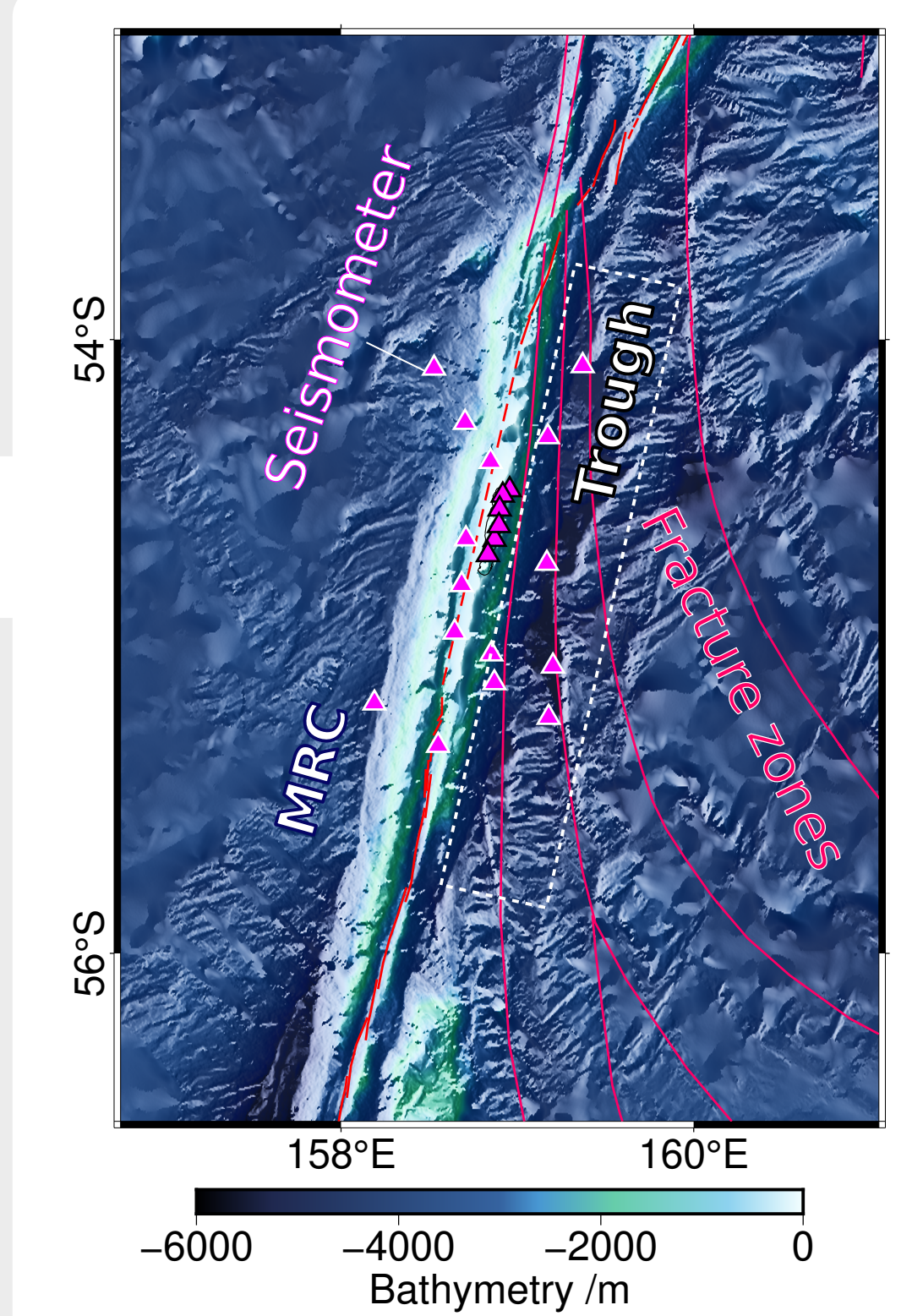


Figure 2 Bathymetric^[4,5,6] features and seismometer locations (black outline→land; white→OBSS) around the Macquarie segment.

4. Interpretations

High density of fracture zones on eastern block provide pathways for **deep lithospheric hydration**^[12], so the velocity contrast likely reflects a difference in fracture density and hydration across the **plate boundary** (Fig. 7), which tracks this segment's tectonic history as previously being an oblique spreading ridge cut by numerous transform faults^[1].

High fracture density leads to **mechanical instability** in the Pacific plate and a **wet lithosphere** favours **megathrust development**^[13]. Therefore **westward subduction** of the Pacific may become possible.

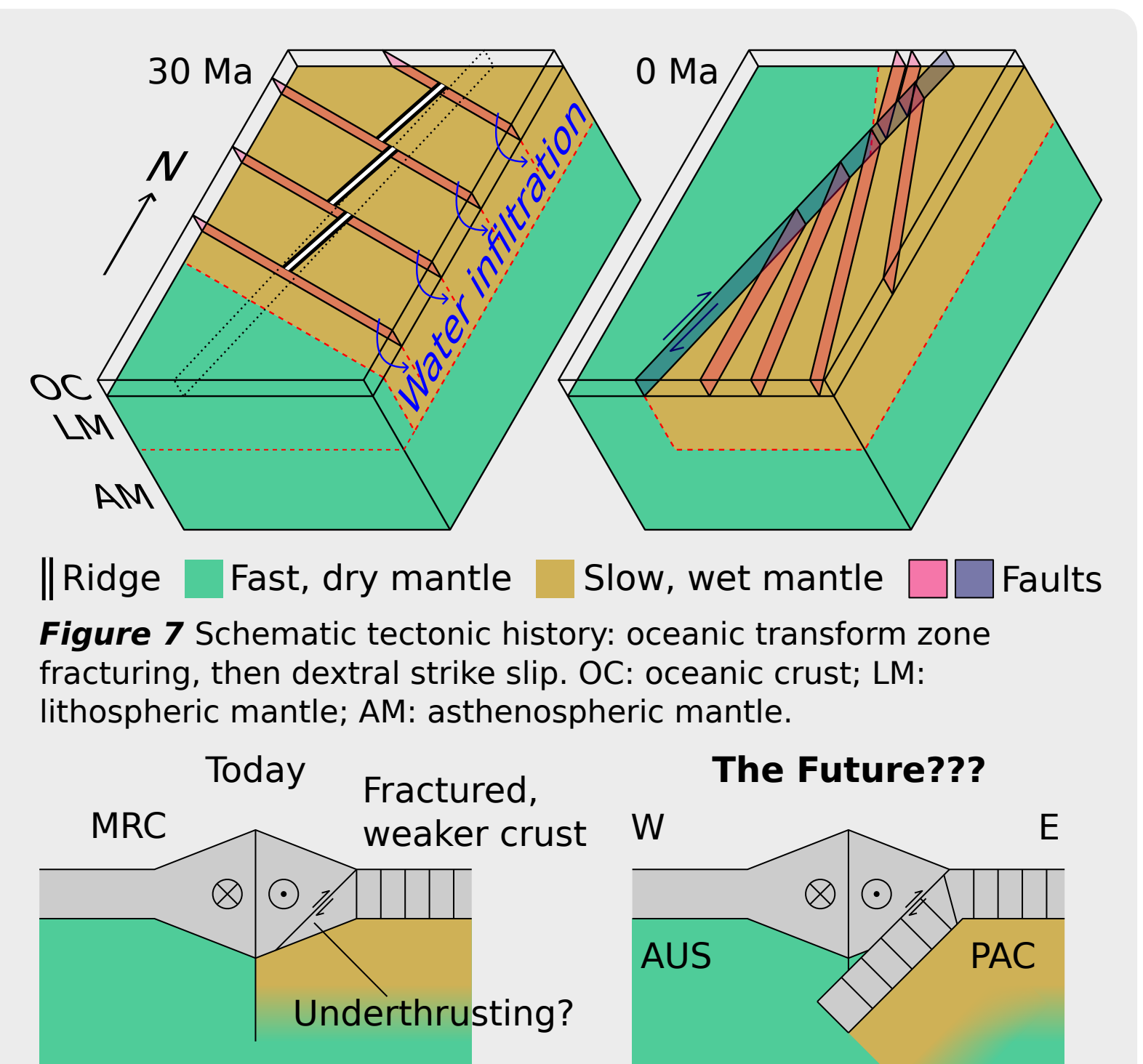


Figure 7 Schematic tectonic history: oceanic transform zone fracturing, then dextral strike slip. OC: oceanic crust; LM: lithospheric mantle; AM: asthenospheric mantle.
 Figure 8 E-W cross sections speculating on the future of Macquarie Island? A wet lithosphere promotes the development of a lithospheric-scale localised shear zone, potentially leading to incipient subduction. AUS: Australian plate; PAC: Pacific plate.

5. Future Work

A **local earthquake catalogue** with accurate locations and focal mechanisms can provide further insights. Are there any **reverse faults** arranged along a **thrust plane**? Or is seismicity principally hosted by **strike slip** faults along **subvertical fault planes**?
 The nature of local seismicity can determine whether the **low convergence angle** or the **compositional contrast** is the primary control of the PAC-AUS boundary along the Macquarie segment.

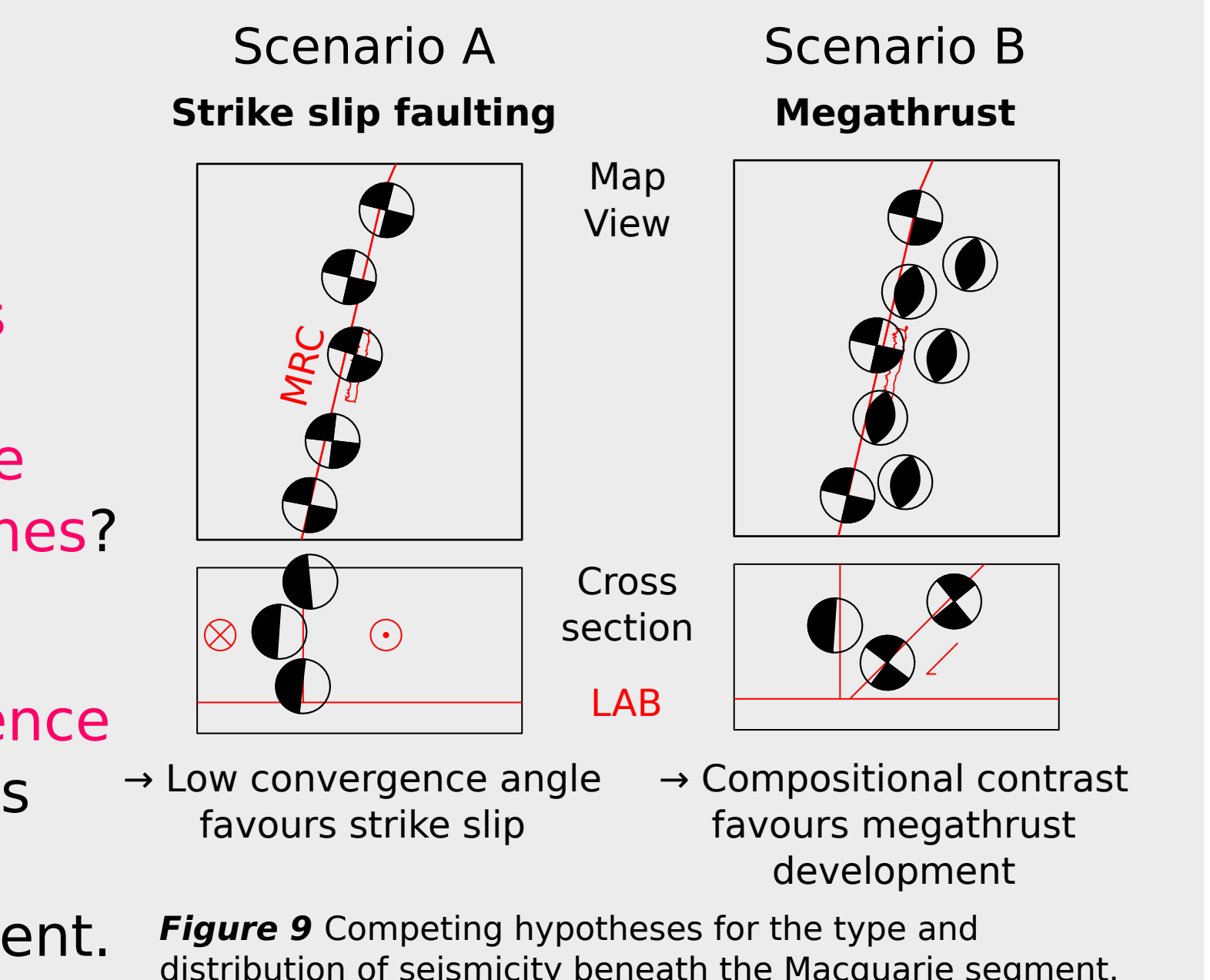


Figure 9 Competing hypotheses for the type and distribution of seismicity beneath the Macquarie segment.

6. Conclusions

A collection of **denoised waveforms** images the lithospheric **velocity structure** beneath Macquarie Island. **Low velocity hydrated** Pacific lithospheric mantle is placed against **unhydrated** Australian oceanic lithosphere in a configuration that will not hinder **westward subduction**. However, the **current status** of the plate boundary along the Macquarie segment remains **uncertain**, which we hope to resolve using a **local earthquake catalogue**.

References

[1] Jiang et al. (2021). Timing of seafloor spreading cessation at the Macquarie Ridge Complex (SW Pacific) and implications for upper mantle heterogeneity. G-Cubed. DOI: 10.1029/2020GC009485
 [2] Meckel et al. (2005). Influence of cumulative convergence on lithospheric thrust fault development and topography along the Australian-Pacific plate boundary south of New Zealand. G-Cubed. DOI:10.1029/2005GC000914
 [3] Shuck et al. (2021). Strike-slip enables subduction initiation beneath a failed rift: New seismic constraints from Puysegur Margin, New Zealand. Tectonics. DOI:10.1029/2020TC006436
 [4] The GEBCO 2025 Grid - a continuous terrain model for oceans and land at 15 arc-second intervals. DOI:10.5285/37C529E6-24EA-67CE-E063-7086A6BC05F29
 [5] Mosher & Symons (2008). Ridge reorientation mechanisms: Macquarie Ridge Complex, Australia-Pacific plate boundary. Geology. DOI:10.1130/G24236A.1
 [6] Daczko et al. (2003). Extension along the Australian-Pacific transpressional transform plate boundary near Macquarie Island. G-Cubed. DOI:10.1029/2003GC000523
 [7] Tkalčić et al. (2020). https://www.fdsn.org/networks/detail/3f_2020/
 [8] Janiszewski et al. (2019). An amphibious surface-wave phase-velocity measurements of the Cascadia subduction zone. GJI. DOI:10.1093/gji/ggz051
 [9] Audet & Janiszewski (2020). OBSTools (Python Package). DOI:10.5281/ZENODO.4281480
 [10] Rawlinson & Kennett (2004). Rapid estimation of relative and absolute delay times across a network by adaptive stacking. GJI. DOI:10.1111/j.1365-246X.2004.02188.x
 [11] International Seismological Centre (2025). ISC Bulletin. DOI:10.31905/D0808B30
 [12] Wang et al. (2022). Deep hydration and lithospheric thinning at oceanic transform plate boundaries. Nat. Geosci. DOI:10.1038/s41561-022-01003-3
 [13] Regenauer-Lieb et al. (2001). The Initiation of Subduction: Criticality by Addition of Water?. Science 294, 578-580. DOI:10.1126/science.1063891

YL is supported by the NERC grant number NE/S007164/1